Spreading Depolarization during the Acute Stage of Experimental Subarachnoid Hemorrhage in Mice

Zelong Zheng, Michael Schoell, Renan Sanchez-Porras, Christian Diehl, Andreas Unterberg, and Oliver W. Sakowitz

Abstract Spreading depolarization (SD) has been suggested as a pathomechanism for delayed cerebral ischemia after subarachnoid hemorrhage (SAH). However, the role of SD during the acute phase of SAH is still unclear. The objective of this study was to investigate (a) the occurrence of SD with intrinsic optical signal (IOS) imaging, (b) the effect of ketamine on SD, and (c) the resulting brain edema (brain water content (BWC)) during the acute stage of experimental SAH in mice. SAH was elicited by the endovascular filament perforation method. After SAH or sham operation, ketamine or saline, 30 mg/kg, was given every half hour. Changes in tissue light reflectance were recorded with IOS. BWC was measured during the acute stage. Overall, 199 SDs occurred in SAH groups and 33 SDs appeared in sham groups. These SDs displayed distinct originating and spreading patterns. Compared with saline, ketamine decreased SD spread and influenced the amplitude, duration, and speed of SD. However, the occurrence of SD was not prevented by ketamine. Moreover, ketamine did not reduce BWC after SAH. These results demonstrate that SD occurs with a high incidence during the acute stage of SAH. SDs are heterogeneous in incidence, origination, and propagation. It remains unclear whether ketamine effects on SD may be viewed as therapeutically beneficial after SAH.

Introduction

Spreading depolarization (SD) is a near-complete depolarization wave of neuronal and glial cells in the gray matter of central nervous system, propagating at 2–5 mm/min [6, 14]. A main feature of these waves is a remarkable breakdown of ion gradients between extra- and intracellular spaces, which favors neuronal swelling and dendrite distortion due to an osmotic imbalance [14]. For the restoration of ion hemostasis, SD is accompanied by an increase of energy metabolism with a pronounced utilization of oxygen and an increase of the regional cerebral blood flow (rCBF). Under conditions of anoxia and ischemia, the hemodynamic response to SD is sometimes inverted to a marked, prolonged hypoperfusion initiated by the severe vasoconstriction [6]. This perfusion deficit is so severe that it markedly elevates metabolic stress and is capable of inducing brain damage.

Subarachnoid hemorrhage (SAH) resulting from intracranial aneurysmal rupture is associated with a high morbidity and mortality [22]. Early brain injury, activated at aneurysm rupture, evolves with time and has been considered as one of important factors determining the prognosis of SAH [21]. Currently, SD was reported to occur during the early phase of SAH in clinical and experimental studies. Hubschmann et al. [11] recorded cellular depolarization waves with ECoG and ion-specific microelectrodes in a cat SAH model and suggested that SAH generated a primary cellular dysfunction capable of inducing SD during the acute phase. In another study, Beaulieu et al. [4] detected SD in rat cortex after SAH using diffusion-weighted MRI. They concluded that the occurrence of SD was a consequence of the acute hemorrhage process during SAH. Moreover, Van Den Bergh et al. [24] found that prolonged depolarizations occur immediately after SAH in a rat

Z. Zheng (✉)
Department of Neurosurgery, Heidelberg University Hospital, Heidelberg, Germany

Department of Neurosurgery, Guangzhou First People's Hospital, School of Medicine, South China University of Technology, Guangzhou, China

M. Schoell
Institute for Medical Biometry and Informatics, Heidelberg University, Heidelberg, Germany

R. Sanchez-Porras · C. Diehl · A. Unterberg · O. W. Sakowitz
Department of Neurosurgery, Heidelberg University Hospital, Heidelberg, Germany

model and the duration of SD was associated with the extent of ischemic lesions. Additionally, multicenter, retrospective clinical studies have demonstrated that SD appeared during the early phase of SAH [7, 18]. However, until now, little information about SD during the acute phase of SAH is known.

Intrinsic optical signal (IOS) imaging is a functional neuroimaging technique that enables the visualization of optical reflectance changes at the brain surface [3]. IOS allows for fine temporal and spatial resolution (i.e., seconds and micrometer). It is particularly appropriate for the study of SD because a large region of cortex can be studied simultaneously and multiple time points can be collected over time as the depolarization spreads.

Here, we investigated SD incidence, the effect of ketamine on SD, and the dynamic of the spatial-temporal patterns of SD with IOS during the acute phase of SAH. Moreover, acutely developing brain edema was studied at 3 h after SAH. Meanwhile, intracranial pressure (ICP) was monitored.

Materials and Methods

Forty-eight male C57Bl6 mice (23–25 g body weight; Charles River Laboratory, Sulzfeld, Germany) (Fig. 1) were used for experiments approved by the authorities in animal research in Baden-Württemberg (Protocol Number 35-9185.81/G-203/12).

Experimental Animals and Monitoring

Animals had free access to food and water prior to surgery. Anesthesia was induced by intraperitoneal injection with a threefold combination of midazolam (5 mg/kg), fentanyl (0.05 mg/kg), and medetomidine (0.5 mg/kg) and maintained by hourly injections of one-third of the initial dose. Animals were intubated and mechanically ventilated with 50% oxygen and 50% nitrogen (Minvent Type 845, Hugo Sachs Elektronik Harvard Apparatus GmbH, March, Germany). The left femo-

ral artery was cannulated for continuous blood pressure measurement, blood sample collection, and fluid administration. The body temperature was recorded by a rectal thermometer (LSI, Letica Scientific Instruments, Barcelona, Spain) and kept constantly at 37 °C by a servo-controlled heating pad.

ICP was continuously measured from 40 min before until 3 h after SAH in the parenchyma of the left hemisphere using a Codman ICP microsensor (Johnson & Johnson Medical Limited, Berkshire, UK).

Induction of Subarachnoid Hemorrhage

After the right carotid artery was exposed with careful conservation of the vagus nerve, a 5-0 nylon monofilament was advanced via the external carotid artery (ECA) into the internal carotid artery (ICA). Then the filament was pushed forward until a massive ICP increase was observed. This was the sign of perforation and SAH. After observing ICP increase, the filament was withdrawn immediately into the stump of ECA, and then the vessel was closed by means of ligature. Then the wound was sutured.

Assessment of Brain Water Content

Animals were sacrificed 3 h after induction of SAH. The olfactory bulb and the cerebellum were removed, and the wet weight (WW) of the brain was assessed. Thereafter, the brain was dried for 24 h at 110 °C and their dry weight (DW) was determined. Brain water content (%) was calculated using the following formula $[(WW - DW)/WW] \times 100$.

IOS Acquisition

The mouse's head was illuminated by two LED white-light sources. A CCD camera (Smartec GC1621M, 8 bit gray-
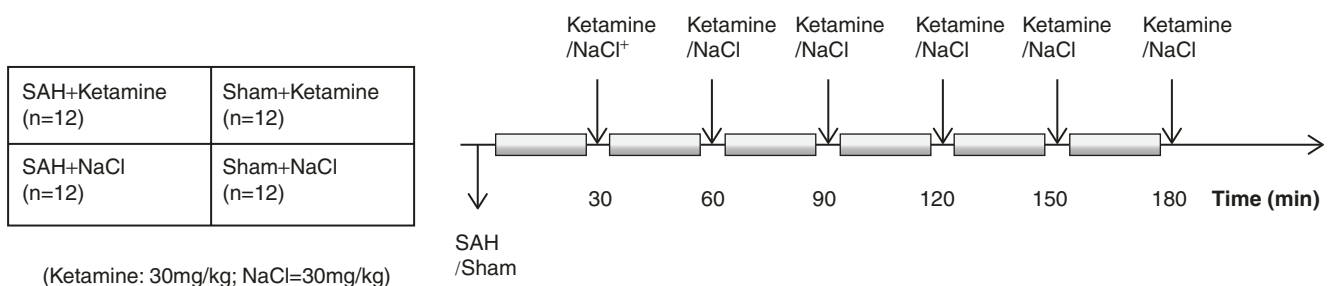

Fig. 1 Schematic design of the current study for IOS after SAH. Animals were randomly assigned into SAH and sham groups. After SAH or sham operation, they were given ketamine or saline every 30 min until 180 min later

scale, 1628 × 1236 pixels, Maxx Vision GmbH, Stuttgart, Germany) was mounted above the thinned skull and connected to a computer. An optical band-pass filter (564 nm, 10 nm FWHM) in front of the camera selected the desired wavelength. Image acquisition was performed until 3 h after induction of SAH at a rate of two images per second at 700 × 600 resolutions to fit the size of mouse's head. Images were saved onto a hard disk for later processing.

Data Analysis

IOS images were elastically registered to a manually chosen reference image. The registration procedure was to reduce movement artifacts of the cortex induced by breathing and heartbeat.

For each experiment, ten regions of interest (ROIs) with 5 × 5 pixels in size distributed along one hemisphere were selected. Similar locations for ROIs were chosen in all of the experiments by taking anatomical landmarks, such as skull sutures and large vessels, to identify similar locations. Custom-written software based on ImageJ was used to inspect the large amounts of images and to identify relevant ROIs. The intensity profiles extracted from the ROIs at identified time points were then analyzed in Labchart software. After obtaining a baseline intensity value, the amplitude was achieved. The duration of intensity changes and the speed and number of ROIs reached per SD were also measured. The cortex area touched per SD was also analyzed with our software. Aided by the parameter images of maximal and minimal intensity changes during SD, the manually selected expansion area gave the absolute visible area of expansion of SD. To compare the expansion areas between different animals, these areas were normalized by the whole visible cortex area, for each mouse. This resulted in the percentage of visible cortex covered by a specific SD.

Statistical Analysis

Descriptive statistics were calculated for all outcome variables of interest. All data are presented as means±standard error of the mean (SEM), if not indicated otherwise. To test differences in means and numbers of events, independent sample Student's t-test and Mann-Whitney tests were used. All statistical tests were performed two-sided, and the statistical significance was assumed as $p < 0.05$. For statistical analysis SPSS 20.0 for Windows (SPSS Inc., Chicago, Illinois, USA) was used.

Results

Physiological Parameters

The mean arterial pressure, rectal temperature, and arterial blood gases were in the normal range before induction of SAH (Table 1).

Observation of SD

A total of 199 SDs occurred in animals with SAH (8.3 SD per animal), while, interestingly, 33 SDs also occurred in sham groups (1.4 SD per animal) (Mann-Whitney U-test: $p < 0.01$ vs. sham). Most of SD appeared within 30–60 min (42.6%) after SAH, which means that SAH leads to immediate SD.

Spatiotemporal Patterns of SD

SD had different originating sites, propagation direction, and patterns (Fig. 2) in the cerebral cortex of mice after SAH.

Originating Sites
The originating sites of SD were classified into three types: the cerebral cortex adjacent to the ICP sensor, other area of the cerebral cortex, and the olfactory bulb. After SAH, 48 SDs initiated from the cerebral cortex next to the ICP sensor, 115 SDs came from other parts of the cerebral cortex, and 36 SDs originated from the olfactory bulb.

Initiation and Propagation Patterns
Radial wave: These waves originated from a single point, and their wave front diverged in all directions, assuming a

Table 1 The result of blood gas analysis before SAH induction or sham surgery

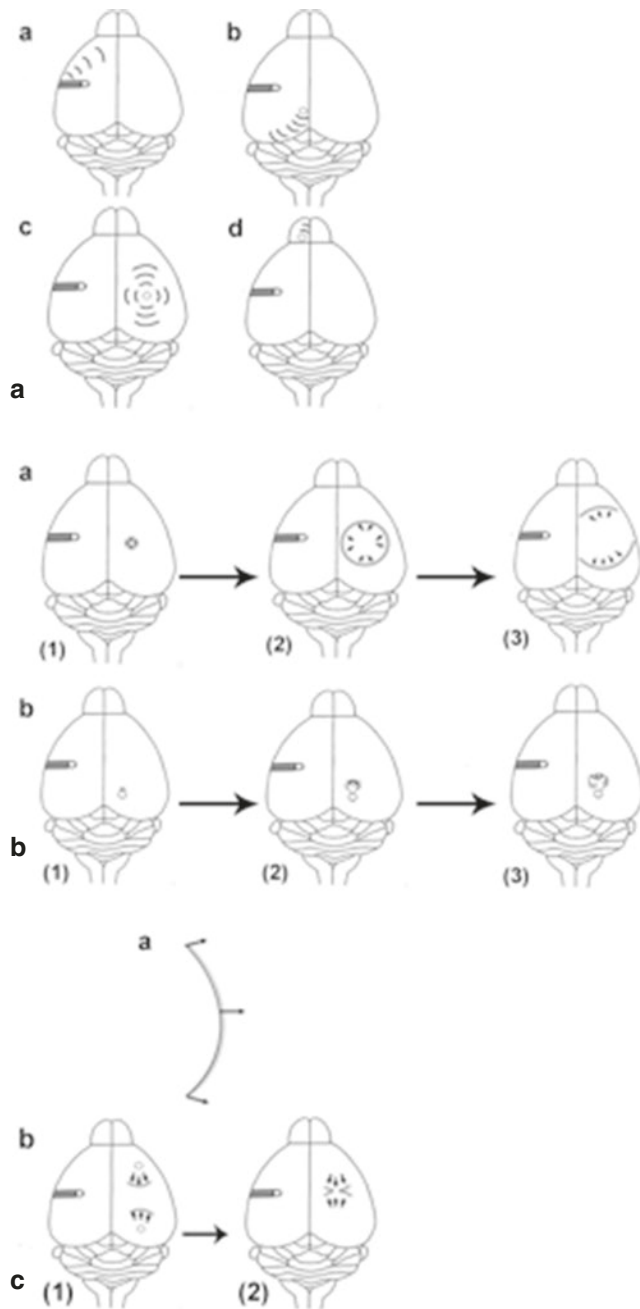|	pH	pO$_2$	pCO$_2$	HCO$_3^-$	Na$^+$	K$^+$	Cl$^-$	Ca^{2+}
SAH + ketamine	7.29 ± 0.01	92.2 ± 1.8	40.5 ± 0.8	19.0 ± 0.2	147.45 ± 0.50	4.6 ± 0.1	119.5 ± 0.7	0.94 ± 0.04
Sham+ketamine	7.32 ± 0.01	96.2 ± 1.0	40.3 ± 0.4	19.7 ± 0.2	147.00 ± 0.49	4.4 ± 0.1	116.8 ± 0.5	1.04 ± 0.02
SAH + NaCl	7.32 ± 0.01	92.2 ± 1.1	39.1 ± 0.9	19.3 ± 0.3	147.22 ± 0.58	4.4 ± 0.1	117.9 ± 0.7	1.00 ± 0.02
Sham+NaCl	7.31 ± 0.01	96.2 ± 0.7	40.3 ± 0.4	19.2 ± 0.2	146.68 ± 0.64	4.3 ± 0.1	116.7 ± 0.7	0.99 ± 0.01

Fig. 2 Spatiotemporal patterns of SD after SAH. Origins of spontaneous SDs (**A**) distributed on different locations of the brain: the cerebral cortex adjacent to the ICP sensor (**A***a*), other cerebral cortex in the contralateral hemisphere (**A***b*) or the ipsilateral hemisphere (**A***c*), and the olfactory bulb (**A***d*). And SD initiates with radial (**B***a1*) or irregular radial pattern (**B***b1*). The most common initiation pattern in the current study is the irregular radial pattern. It expands and creates a solitary broken radial wave (*b2–3*). The radial wave of SD forms two semi-planar waves when it encounters vessels or fissures (a2–3). All SDs evolve into semi-planar waves (**C***a*). When two wave fronts collide, they interact and may annihilate (**C***b1–2*)

spherical shape. Waves may then "break" at some time points when hampered, forming two or more semi-planar waves.

Irregular radial wave: These waves began as a radial wave from the origination point expanding asymmetrically during the early spreading phase, breaking the integrated circle. Wave fronts could develop into a single semi-planar wave.

There were 186 SDs (93.5%) initiating as irregular radial waves and 13 SDs (6.5%) originating as radial waves after SAH.

Semi-planar wave: Waves with a flat-rounded front preserve some radial direction and have two open ends, traveling in one direction.

Collision: When two wave fronts collide, they can annihilate because of the resistance of the excitable medium.

One hundred and ninety-nine SDs quantified in all experiments spread in a semi-planar fashion. The morphology of SD waves was affected by the surface of the cerebral cortex, the presence of ICP sensors, and other SDs. When two SDs wave fronts encountered each other, they interacted and collided.

Effect of Ketamine on SD

After SAH, 91 SDs occurred in animals treated with ketamine, and 108 SDs appeared in saline-treated animals (Mann-Whitney U-test: $p = 0.775$). ROIs reached by SD was 3.2 ± 0.3 in ketamine-treated SAH animals and 3.8 ± 0.3 in saline-treated SAH group (Mann-Whitney U-test: $p < 0.05$). After SAH, the speed of SD between ketamine-treated and saline-treated groups significantly differed (2.7 ± 0.1 mm/min vs. 3.3 ± 0.1, independent sample Student's t-test, $p < 0.01$). The area covered by SD was $14.4 \pm 1.5\%$ in ketamine-treated mice with SAH and $19.0 \pm 1.7\%$ in saline-treated animals with SAH (Mann-Whitney U-test, $p < 0.01$). Moreover, the intensity change between these two groups was also significantly different ($7.7 \pm 0.6\%$ vs. $9.9 \pm 0.5\%$, Mann-Whitney U-test, $p < 0.001$). In addition, the interval time among SDs was 21.2 ± 3.1 min in the ketamine-treated SAH group, whereas, in the saline-treated mice with SAH, the interval was significantly lower at 11.9 ± 1.1 min.

Brain Water Content

After SAH, the brain water content at 3 h was $80.2 \pm 0.6\%$ vs. $79.6 \pm 0.3\%$ in sham-operated animals (independent sam-
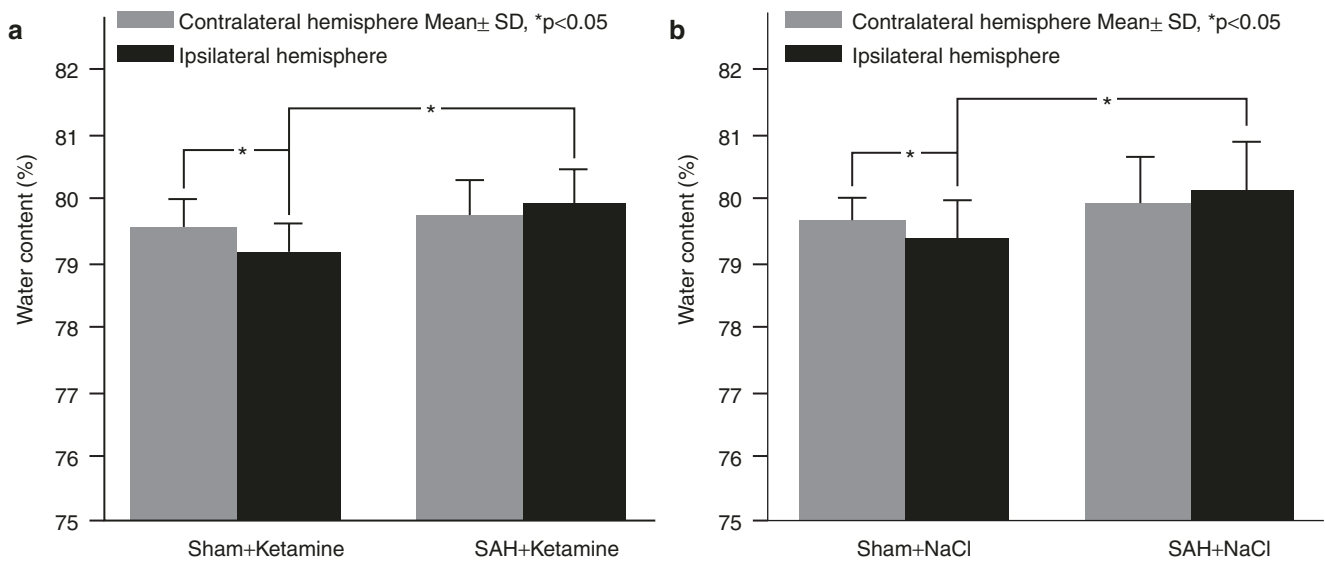
Fig. 3 Total brain water content (BWC) after SAH or sham surgery: the water content in ketamine-treated (**a**) and saline-treated (**b**) SAH or sham groups. BWC of SAH groups is higher than that of sham groups, and in sham groups, BWC of contralateral hemispheres significantly increases. The data is expressed as mean ± standard deviation

ple Student's t-test, $p < 0.05$). Although brain water content in ketamine-treated animals (79.8 ± 0.1%) was lower than in saline-treated groups (79.9 ± 0.1%) after SAH, there was no significant difference (independent sample Student's t-test, $p = 0.683$) (Fig. 3).

Discussion

Using IOS, the incidence of SD during the acute stage (3 h) of SAH was measured, as exemplified by a mouse model. It was found that SD occurred in almost 100% of mice after SAH, which is higher than had been reported following aneurysmal SAH (72%) in patients [7] and similar to that after malignant ischemic stroke (100%) in humans [5]. A possible reason for higher incidence of SD is the recording method: IOS can record SD in large area of cerebral cortex and has high spatiotemporal resolution. However, subdural electrode strips only capture SD that spread across it. In addition, SD during the first 3 hours after SAH cannot be investigated in patients. Furthermore, global brain ischemia exists during the first hour after SAH and coincides with the peak of SD activity at that time.

The results presented by this study also demonstrate that SD is heterogeneous in incidence, origination, and propagation after SAH in mice. SD may originate from the cerebral cortex adjacent to the ICP sensor, olfactory bulb, or other area of the cerebral cortex. As an exception, SD from the olfactory bulb did not spread out of this region. These phenomena would appear at least superficially consistent with the anatomical differences between cerebral cortex and the olfactory bulb. In the olfactory bulb, the susceptibility to SD is low because of GABAergic inhibition [2]. Moreover, the cytoarchitectural separation of the olfactory bulb might provide an explanation for restriction of SD propagation in this area. SDs originating from the cerebral cortex nearby the ICP sensor were most likely induced by the sensor, since it is known that relatively minor mechanical stimuli are able to evoke SD.

SD is regarded as a roughly isotropic and concentric phenomenon; however, we found that expansion patterns of SD after SAH in mice were different. As we know, the truly concentric and isotropic SD is observed in chicken retina, which has a uniform, avascular structure [15]. This implies that the heterogeneity of SD in cerebral cortex may be due to ununiformed cellular and vascular structures. In our study, most of SD with the radial pattern appear in the ipsilateral hemisphere. As we know, The origin sites of radial pattern SD are areas with apparent reduced perfusion because of accumulation of K^+ and ischemia after SAH [19]. The ipsilateral hemisphere suffers more serious ischemic damage than contralateral one after SAH [23], in which accumulation of $[K^+]_o$ and ischemia can appreciate the area with marked decreased perfusion, observed in SD with radial patterns.

Furthermore, the present study underscores that ketamine with the dosage of 30 mg/kg has the capacity to suppress SD propagation and reduce SD amplitude and duration in mouse

SAH model. However, SD induction is not prohibited. Moreover, ketamine does not reduce brain edema at 3 h after SAH. As a noncompetitive antagonist, ketamine can bind at the phencyclidine site and thus decrease the channel opening time and the amplification of the response to a repeated stimulation. In addition, ketamine is capable of binding in one site located in the hydrophobic domain of the NMDA receptor where it decreases the frequency of channel opening [20]. Therefore, ketamine is capable of modulating SD properties. Other experimental studies also report that SD is blocked by ketamine at significantly high doses in diverse lissencephalic animal models [1, 13]. In addition, ketamine at dosage used in human can prevent SD induced by KCl stimulation in the gyrencephalic swine brain [17]. However, those studies were carried out in physiological conditions, and the effect of ketamine on SD may be different in pathological situations. In the current study, SD induction after SAH was not blocked by ketamine, although it did suppress SD expansion and propagation. Petzold et al. suggested that in pathological conditions, the efficacy of NMDA receptor antagonists was reduced, and they were not able to block SD induced by high extracellular potassium concentration [16]. Conversely, after the MCAO model in rats, delayed (8 h after ischemia) application of an NMDA receptor antagonist reduced infarct volume and the frequency of SDs [8]. Furthermore, clinical studies demonstrated that ketamine decreased SD incidence in patients with brain injury [10, 18]. It may be implied that the occurrence of SD is related to both different intensities between conditions and usage of NMDA receptor antagonists; if the effect of the deleterious condition is stronger than the NMDA receptor antagonist, SD will occur despite the presence of the drug in the region exposed to the deleterious condition [9]. Additionally, the blocking effect of ketamine on SD is also dependent on used dosage and administration route. In the present study, a subanesthetic dosage of 30 mg/kg was used through intraperitoneal injection, but SDs were not blocked. Ketamine may be able to block SD completely through intravascular infusion or increasing the dosage. As shown by Sanchez-Porras et al., ketamine infusion at 2 mg/kg/h was not able to inhibit SD induction but prevented its expansion, whereas at 4 mg/kg/h, SDs were fully blocked [17]. Until now, there has been limited evidence available regarding clinical benefits after the administration of ketamine. The low dosage of ketamine and occult adverse effects may contribute to this failure in patients with brain injury [12]. However, ketamine still exhibits a neuroprotective potential, and it is necessary to carry on more experimental studies in proper animal models and prospective clinical trials in patients with deleterious conditions to clarify the effect of ketamine on SD in pathophysiological condition and to establish optimal dosages and administration routes.

Conflict of Interest

None.

References

1. Amemori T, Bures J. Ketamine blockade of spreading depression: rapid development of tolerance. Brain Res. 1990;519:351–4.
2. Amemori T, Gorelova NA, Bures J. Spreading depression in the olfactory bulb of rats: reliable initiation and boundaries of propagation. Neuroscience. 1987;22:29–36.
3. Ba AM, Guiou M, Pouratian N, Muthialu A, Rex DE, Cannestra AF, Chen JW, Toga AW. Multiwavelength optical intrinsic signal imaging of cortical spreading depression. J Neurophysiol. 2002;88:2726–35. https://doi.org/10.1152/jn.00729.2001.
4. Beaulieu C, Busch E, de Crespigny A, Moseley ME. Spreading waves of transient and prolonged decreases in water diffusion after subarachnoid hemorrhage in rats. Magn Reson Med. 2000;44:110–6.
5. Dohmen C, Sakowitz OW, Fabricius M, Bosche B, Reithmeier T, Ernestus RI, Brinker G, Dreier JP, Woitzik J, Strong AJ. Spreading depolarizations occur in human ischemic stroke with high incidence. Ann Neurol. 2008;63:720–8.
6. Dreier JP. The role of spreading depression, spreading depolarization and spreading ischemia in neurological disease. Nat Med. 2011;17:439–47. https://doi.org/10.1038/nm.2333.
7. Dreier JP, Woitzik J, Fabricius M, Bhatia R, Major S, Drenckhahn C, Lehmann T-N, Sarrafzadeh A, Willumsen L, Hartings JA. Delayed ischaemic neurological deficits after subarachnoid haemorrhage are associated with clusters of spreading depolarizations. Brain. 2006;129:3224–37.
8. Hartings JA, Rolli ML, X-CM L, Tortella FC. Delayed secondary phase of peri-infarct depolarizations after focal cerebral ischemia: relation to infarct growth and neuroprotection. J Neurosci. 2003;23:11602–10.
9. Hernández-Cáceres J, Macias-González R, Brožek G, Bureš J. Systemic ketamine blocks cortical spreading depression but does not delay the onset of terminal anoxic depolarization in rats. Brain Res. 1987;437:360–4.
10. Hertle DN, Dreier JP, Woitzik J, Hartings JA, Bullock R, Okonkwo DO, Shutter LA, Vidgeon S, Strong AJ, Kowoll C, Dohmen C, Diedler J, Veltkamp R, Bruckner T, Unterberg AW, Sakowitz OW. Effect of analgesics and sedatives on the occurrence of spreading depolarizations accompanying acute brain injury. Brain. 2012;135:2390–8. https://doi.org/10.1093/brain/aws152.
11. Hubschmann OR, Kornhauser D. Cortical cellular response in acute subarachnoid hemorrhage. J Neurosurg. 1980;52:456–62. https://doi.org/10.3171/jns.1980.52.4.0456.
12. Ikonomidou C, Turski L. Why did NMDA receptor antagonists fail clinical trials for stroke and traumatic brain injury? The Lancet Neurology. 2002;1:383–6.
13. Krüger H, Heinemann U, Luhmann HJ. Effects of ionotropic glutamate receptor blockade and 5-HT1A receptor activation on spreading depression in rat neocortical slices. Neuroreport. 1999;10:2651–6.
14. Lauritzen M, Dreier JP, Fabricius M, Hartings JA, Graf R, Strong AJ. Clinical relevance of cortical spreading depression in neurological disorders: migraine, malignant stroke, subarachnoid and intracranial hemorrhage, and traumatic brain injury. J Cereb

Blood Flow Metab. 2011;31:17–35. https://doi.org/10.1038/jcbfm.2010.191.

15. Martins-Ferreira H, Nedergaard M, Nicholson C. Perspectives on spreading depression. Brain Res Rev. 2000;32:215–34.

16. Petzold GC, Windmüller O, Haack S, Major S, Buchheim K, Megow D, Gabriel S, Lehmann T-N, Drenckhahn C, Peters O. Increased extracellular K+ concentration reduces the efficacy of N-methyl-D-aspartate receptor antagonists to block spreading depression-like depolarizations and spreading ischemia. Stroke. 2005;36:1270–7.

17. Sánchez-Porras R, Santos E, Schöll M, Stock C, Zheng Z, Schiebel P, Orakcioglu B, Unterberg AW, Sakowitz OW. The effect of ketamine on optical and electrical characteristics of spreading depolarizations in gyrencephalic swine cortex. Neuropharmacology. 2014;84:52–61.

18. Sakowitz OW, Kiening KL, Krajewski KL, Sarrafzadeh AS, Fabricius M, Strong AJ, Unterberg AW, Dreier JP. Preliminary evidence that ketamine inhibits spreading depolarizations in acute human brain injury. Stroke. 2009;40:e519–22. https://doi.org/10.1161/strokeaha.109.549303.

19. Santos E, Schöll M, Sánchez-Porras R, Dahlem MA, Silos H, Unterberg A, Dickhaus H, Sakowitz OW. Radial, spiral and reverberating waves of spreading depolarization occur in the gyrencephalic brain. NeuroImage. 2014;99:244–55.

20. Schmid RL, Sandler AN, Katz J. Use and efficacy of low-dose ketamine in the management of acute postoperative pain: a review of current techniques and outcomes. Pain. 1999;82:111–25.

21. Sehba FA, Hou J, Pluta RM, Zhang JH. The importance of early brain injury after subarachnoid hemorrhage. Prog Neurobiol. 2012;97:14–37. https://doi.org/10.1016/j.pneurobio.2012.02.003.

22. Serrone JC, Maekawa H, Tjahjadi M, Hernesniemi J. Aneurysmal subarachnoid hemorrhage: pathobiology, current treatment and future directions. Expert Rev Neurother. 2015;15:367–80. https://doi.org/10.1586/14737175.2015.1018892.

23. Thal SC, Sporer S, Klopotowski M, Thal SE, Woitzik J, Schmid-Elsaesser R, Plesnila N, Zausinger S. Brain edema formation and neurological impairment after subarachnoid hemorrhage in rats: laboratory investigation. J Neurosurg. 2009;111:988–94.

24. van den Bergh WM, Zuur JK, Kamerling NA, van Asseldonk JT, Rinkel GJ, Tulleken CA, Nicolay K. Role of magnesium in the reduction of ischemic depolarization and lesion volume after experimental subarachnoid hemorrhage. J Neurosurg. 2002;97:416–22. https://doi.org/10.3171/jns.2002.97.2.0416.